StitchSwitch: Programmable Surface Deformation and Bistability in Embroidered Textiles

Vivian Li
Brown University
Providence, Rhode Island, USA
vivian_li1@brown.edu

Milin Kodnongbua
University of Washington
Seattle, Washington, USA
milink@cs.washington.edu

Heather Robertson
Brown University
Providence, Rhode Island, USA
heather_robertson@brown.edu

Yiyue Luo
ECE
University of Washington
Seattle, Washington, USA
yiyueluo@uw.edu

Adriana Schulz
Computer Science Department
Brown University
Providence, Rhode Island, USA
adriana_schulz@brown.edu

Abstract

Programming 3D surface deformation has been widely explored in rigid and semi-rigid materials, but achieving predictable shape change in wearable textiles remains challenging. We present StitchSwitch, a computational design and fabrication system for programming surface deformation and bistability into embroidered textiles through a continuous parametric tessellation design space. Embroidering triangle-tessellated patches onto pre-stretched elastic fabric encodes out-of-plane deformation and passive bistability directly into the textile.

We characterize how patch diameter and embroidery fill percentage govern deformation, revealing varied deformation outcomes and a saturation regime where increasing density shifts deformation from vertical height to lateral distribution. We develop a reduced-space simulation model predicting this relationship in real time, integrated into a garment-scale design tool supporting live 3D preview, inverse design, and fabrication-aware export.

We demonstrate StitchSwitch through two garment-integrated applications, a tactile garment interface and a deformation-based storage pocket, showing how programmable bistable deformation enables functional structures directly within textiles.

CCS Concepts

• **Human-centered computing → Interaction devices**.

Keywords

shape-change, programmable textiles, machine embroidery, bistability, computational design, digital fabrication

ACM Reference Format:
Vivian Li, Milin Kodnongbua, Heather Robertson, Yiyue Luo, and Adriana Schulz. 2026. StitchSwitch: Programmable Surface Deformation and Bistability in Embroidered Textiles. In *The 39th Annual ACM Symposium on User Interface Software and Technology (UIST '26), November 02–05, 2026, Detroit, MI, USA.* ACM, New York, NY, USA, 8 pages. https://doi.org/10.1145/3830398.3830499

UIST '26, Detroit, MI, USA

ACM ISBN 979-8-4007-2856-3/26/11
https://doi.org/10.1145/3830398.3830499

1 Introduction

Embedding mechanical behavior directly into materials enables structures that change shape, respond to interaction, and maintain stable configurations without continuous energy input. Bistability, where a structure reversibly switches between two stable states, is a powerful design primitive for interaction, sensing, and adaptive structures, spanning soft interfaces, wearables, and responsive surfaces. Bringing these capabilities to textiles is appealing, since they enable wearable interfaces that stay comfortable while supporting functional behaviors.

Machine embroidery presents an attractive approach because it is digitally programmable, accessible, and compatible with textile workflows. Its ability to incorporate conductive threads further enables sensing and interaction. Stitching onto pre-stretched elastic fabric selectively constrains regions of the material, creating deformation upon release. This work builds on this mechanism to enable continuous, surface-scale control over bistable deformation.

While this mechanism is simple and accessible, it is difficult to design without understanding how embroidery parameters shape the resulting deformation. Embrogami [10] establishes the foundational concept of shape-changing embroidery using a library of 12 discrete primitive structures (6 linear, 6 radial), each individually characterized so its deformation outcome can be mapped directly by linear regression. This approach captures localized shape changes well, but does not extend to the broader, continuous surface-scale control that a single unified parameter space would provide. This gap between a fixed primitive library and continuous design needs limits the usability of embroidery for programmable textile behavior.

We present StitchSwitch, a computational design and fabrication system that targets a broader design space, enabling predictable, continuous control over passive surface deformation and bistability in textiles. Our key insight is that organizing embroidery into structured triangle-based patterns collapses this space into just two geometric parameters, diameter and fill percentage, configured prior to fabrication. Modeling this continuous space requires our predictive simulation, a key technical contribution.

To make this design space usable, we empirically characterize how patch size and embroidery density relate to deformation, then build a design tool that produces fabrication-ready output through a data-driven simulation enabling live 3D preview of parameter manipulation and inverse design from target deformation.

We evaluate StitchSwitch through two garment-integrated applications, a programmable textile interface with tactile input and a deformation-based pocket, illustrating how programmable deformation supports interaction and functional garment features. We also explore design variations such as patches with spatially varying bistability for shape boundaries around functional elements.

In summary, we make the following contributions:

- A fabrication method programming passive, bistable deformation into embroidered textiles via triangle tessellation on pre-stretched fabric
- An empirical characterization linking patch diameter and fill percentage to deformation, including a saturation effect that bounds practical design
- A reduced-space physical simulation model that predicts deformation from design parameters, storing 1D profiles instead of full meshes to enable real-time preview
- A garment-scale design tool supporting live preview, inverse design, and fabrication-aware export

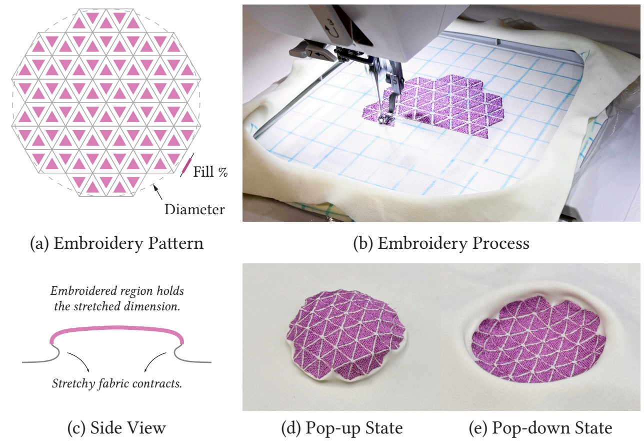

(a) Embroidery Pattern (b) Embroidery Process (c) Side View (d) Pop-up State (e) Pop-down State

Figure 1: StitchSwitch primitive. A triangle-tessellated patch parameterized by diameter and fill percentage (a) is embroidered onto pre-stretched fabric (b). Release induces a tension mismatch that produces bistable deformation (c–e).

2 Related Work

StitchSwitch draws on prior work in shape-morphing structures, textile-based deformation, and computational design of deforming materials, which explore how geometry, material, and fabrication can enable programmable shape change.

Geometry-Driven Shape-Morphing Structures. Foundational work encodes mechanical behavior into geometry to create deployable and bistable structures. Computational frameworks for auxetic surfaces and flexible maps [3, 13–15] use inverse design to map 3D targets to flat patterns, while rod networks and tension-actuated plates [8, 18] induce controlled curvature through geometric constraints. Other work explores programmable morphing and 4D printing [1, 4, 7, 17, 24]. While precise, these approaches often use rigid or semi-rigid materials, such as 3D-printed polymers, that are less suited for wearable textile applications.

Textile-Based Deformation Systems. Other research embeds deformation directly into textile substrates, including through computational knitting [16] and embroidered lace structures [6]. Smocking-based approaches similarly enable computationally designed textile deformation [9, 19, 21]. Systems like OriStitch [2] utilize embroidery to create general 3D geometries but require multi-step fabrication to trigger transformation. Conversely, Embrogami [10] introduces a single-step approach using embroidery on pre-stretched fabric to create bistable fold primitives. Their system characterizes discrete deformation primitives, while StitchSwitch explores a continuous parametric design space where patch geometry and embroidery density can be varied to create surface-scale deformations. This continuous design space enables a broader range of deformation outcomes but requires predictive modeling beyond primitive lookup.

Computational Design of Deforming Systems. To make deformation predictable, systems print tessellated primitives or plastic structures onto pre-stretched fabrics for precision morphological control [5, 11, 12, 23]. While providing structured design spaces, these approaches introduce additional printed material, creating tradeoffs between mechanical properties and fabrication resolution. These pipelines also often rely on simulation-heavy workflows, such as finite element analysis (FEA), to predict deformation. In contrast, StitchSwitch embeds mechanical behavior directly into the fabric through embroidery, leveraging a textile-native process for garment-integrated, washable, reusable structures. Rather than full-mesh simulation, StitchSwitch uses a reduced-space model for real-time preview and inverse design.

3 StitchSwitch Primitive

StitchSwitch programs out-of-plane deformation and bistable switching into soft textiles by embroidering triangle-tessellated patches onto uniformly pre-stretched elastic fabric (Figure 1). Each patch is defined by a circular region filled with a regular tessellation of equilateral triangles at a specified density, forming the basic unit through which deformation is controlled.

The key principle is stiffness encoding: embroidery stitches applied to a pre-stretched substrate locally stiffen the threaded region relative to the surrounding fabric. When released from the hoop, the elastic fabric contracts toward its resting state while the stiffened embroidered patch resists. The mismatch in contraction drives the patch out of plane, producing localized surface deformation. Because the triangle tessellation is highly symmetric, the stitched pattern distributes constraint evenly across the patch, producing balanced, dome-like deformation rather than directional buckling.

This deformation is bistable. When the patch is pressed past a threshold, it snaps between two stable states and remains in either configuration without continued force. Both states are passively maintained by the interplay between the rigidity of the embroidered region and the tension of the surrounding fabric.

The behavior of each patch is controlled by two geometric degrees of freedom: patch diameter and embroidery fill percentage. Fill percentage is defined as the proportion of the patch area covered by stitched triangles and is controlled by uniformly scaling each triangle, introducing gaps between adjacent triangles as fill decreases. Together, these parameters define a compact design space, determining both the magnitude of deformation and the switching behavior between states. We characterize switching force across this design space and find that larger patches and higher fill percentages increase the force required to transition between bistable states, enabling threshold tuning during design.

We fabricate StitchSwitch patches using a standard embroidery machine on pre-stretched elastic fabric with one layer of water-soluble stabilizer. The fabric is uniformly stretched and secured in an embroidery hoop, and the patterns are stitched directly onto the tensioned surface. After embroidery, the fabric is released and the stabilizer is washed away, producing the programmed deformation.

This process is compatible with a range of materials and threads, including conductive threads for functional textile integration. The tessellation enables control over thread distribution, allowing designers to selectively program conductive regions within a patch, varying their amount and placement while preserving the same deformation primitive (Figure 13 in Appendix). Detailed fabrication parameters and materials are provided in Appendix A.

4 Simulation and Characterization

We characterize the design space of triangle-tessellated embroidery patches, focusing on how patch diameter d (in millimeters) and embroidery fill percentage p control deformation behavior and bistable switching, with a simulation calibrated to real-world fabrication. Our key insight for avoiding expensive cloth simulation is to leverage the StitchSwitch pattern's circular symmetry and reduce the full 3D deformation problem to a one-dimensional profile. We model the embroidered fabric as an axis-symmetric membrane whose cross-sectional profile deforms under internal stress induced by the embroidery and elastic fabric. The equilibrium profile minimizes a total elastic energy comprising radial stretching, circumferential stretching, and bending contributions. To encode the mechanical mismatch between embroidered and un-embroidered fabric, the embroidered region is assigned a higher rest-state metric and a different set of stiffness and bending coefficients than the surrounding fabric (Strain and Membrane Energy, below).

Discretization. We represent the fabric as a sequence of nodes $\left(r^{(i)}, z^{(i)}\right)$ parameterized by the undeformed radial coordinate R, where $r^{(i)}$ and $z^{(i)}$ are the radius and the vertical position of the i-th node (Figure 2 (left)). We define stretch factor $\eta = 1.7$, denoting how much the fabric is uniformly stretched during the embroidery process. Patch diameter d is measured on this pre-stretched fabric at the time of embroidery, so dividing by η converts it into the corresponding rest-frame radius, $d/2\eta$, which is what we compare against the undeformed coordinate R throughout. The radial domain is discretized into $N = 300$ nodes, where the resolution is adaptive to make a node lie exactly at the embroidery boundary and the distance between nodes is at most $\Delta R_{\max} = 0.5$mm. Formally, the nodes are at positions $R^{(i)} = i\,\Delta R$, where $\Delta R = (d/2\eta)/N_{\text{in}}$ and $N_{\text{in}} = \lceil (d/2\eta)/\Delta R_{\max} \rceil$. Placing a node exactly on the boundary matters because the fabric's mechanical properties change abruptly there, and this transition is visibly sharp in fabricated samples.

Strain. Writing $r^{(i)}$ and $z^{(i)}$ for the deformed coordinates, we define strain as actual (deformed) length minus rest length, in units of the reference spacing ΔR. Radial strain is the Euclidean distance between consecutive deformed nodes, divided by ΔR, minus the

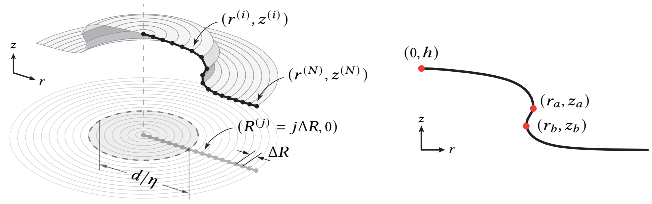

Figure 2: (left) In simulation, we view the fabric as radial strips from the center of the pattern. The deformed fabric is represented by a surface revolution of a one-dimensional profile $r^{(i)}, z^{(i)}$. (right) To capture the characteristics of the profile, we measure three keypoints: the peak height h, the point at the embroidery boundary (r_a, z_a), and the point of minimum radial displacement (r_b, z_b).

segment's rest length $\lambda^{(i)}$ (defined below). Circumferential strain applies the same logic to a ring's circumference: since circumference is always 2π times radius, comparing deformed radius $r^{(i+1)}$ against rest-scaled radius $\lambda^{(i)} R^{(i+1)}$ captures the same stretch without carrying 2π through every term:

$$\varepsilon_r^{(i)} = \max\left(\sqrt{\left(\frac{r^{(i+1)} - r^{(i)}}{\Delta R}\right)^2 + \left(\frac{z^{(i+1)} - z^{(i)}}{\Delta R}\right)^2} - \lambda^{(i)},\ 0\right) \quad (1)$$

$$\varepsilon_\theta^{(i)} = r^{(i+1)} - \lambda^{(i)}\, R^{(i+1)}, \quad (2)$$

where $\lambda^{(i)}$ is the rest-state metric (recall p is embroidery fill percentage), defined as follows:

$$\lambda^{(i)} = \begin{cases} 1 + (\eta - 1)p^2 & \text{if } R^{(i)} \le d/2\eta \text{ (inside)} \\ 1 & \text{otherwise.} \end{cases}$$

Nodes inside the embroidered region are held at pre-stretch factor η, weighted by local fill p^2 since only stitched thread, not the gaps between it, locks in that stretch; nodes outside are ordinary relaxed fabric with $\lambda^{(i)} = 1$. The $\max(\cdot, 0)$ means only stretching is penalized: if a segment is shorter than its rest length, the fabric simply wrinkles out of plane rather than resisting compression, so this costs no energy.

Membrane energy. The membrane energy weights each strain by the circumference at $R^{(i+1)}$:

$$E_{\text{memb}} = \frac{1}{N} \sum_i \left[k_r^{(i)} \left(\varepsilon_r^{(i)}\right)^2 \lambda^{(i)} R^{(i+1)} + \frac{k_\theta^{(i)} \left(\varepsilon_\theta^{(i)}\right)^2}{\lambda^{(i)} R^{(i+1)}} \right], \quad (3)$$

where $k_r^{(i)}$ and $k_\theta^{(i)}$ are piecewise-constant stiffness coefficients that take different values inside and outside the embroidered boundary, interpolating between an embroidery stiffness $k_{*,\text{emb}}$ and a bare-fabric stiffness $k_{*,\text{fab}}$ in proportion to fill percentage, since a sparser tessellation leaves more bare, unstitched fabric between threads. Both $k_{*,\text{emb}}$ and $k_{*,\text{fab}}$ are free parameters calibrated from fabricated samples (see Calibration procedure, below):

$$k_*^{(i)} = \begin{cases} k_{*,\text{emb}} p^2 + k_{*,\text{fab}} (1 - p^2) & \text{if } R^{(i)} \le d/2\eta \text{ (inside)} \\ k_{*,\text{fab}} & \text{otherwise.} \end{cases}$$

Bending energy. Jourdan et al. [11] simulate a similar bilayer mechanism: plastic strips printed onto pre-stretched fabric, where the stiff top layer drives bending upon release, just as our embroidered stitches do. Their full model uses a continuum formulation rather than our reduced profile, but since the same bilayer relationship drives bending in both, we adopt their bending term: the dihedral angle $\theta^{(i)}$ between consecutive surface normals, close to zero for smooth curves and growing as the profile folds more sharply:

$$E_{\text{bend}} = \frac{1}{N} \sum_i w_b^{(i)} \; \frac{(r^{(i+1)})^2}{\bar{r}^{(i)} \, \|\boldsymbol{\ell}^{(i)}\| + \bar{r}^{(i+1)} \, \|\boldsymbol{\ell}^{(i+1)}\|} \; \tan^2\left(\frac{\theta^{(i)}}{2}\right), \tag{4}$$

where $\bar{r}^{(i)} = (r^{(i)} + r^{(i+1)})/2$ is the midpoint radius, $\boldsymbol{\ell}^{(i)}$ the segment vector, and $w_b^{(i)}$ the bending weight (piecewise as above). The factor $(r^{(i+1)})^2/(\bar{r}\|\boldsymbol{\ell}\|)$ is edge length over conical-face surface area, penalizing bending per unit area rather than per node.

Fabric hardening near its stretch limit. We also include a logarithmic term that captures the hardening of knitted fabrics when largely stretched, similar to a rubber band nearing its limit:

$$E_{\log} = \frac{w_{\log}}{N} \sum_i (\varepsilon_\theta^{(i)} - \gamma) \log\left(\frac{\gamma - \varepsilon_\theta^{(i)}}{\gamma}\right) - \varepsilon_\theta^{(i)}, \tag{5}$$

which grows sharply as circumferential strain $\varepsilon_\theta^{(i)}$ approaches a maximum γ, discouraging solutions that over-stretch the fabric beyond what is physically realistic.

Solving for the equilibrium shape. The total energy minimized is

$$E = E_{\text{memb}} + E_{\text{bend}} + E_{\log}, \tag{6}$$

subject to the boundary conditions $r(0) = 0$ and $z'(0) = 0$ (symmetry at the center). A sign constraint $z'(R) \leq 0$ is enforced throughout, forcing the pop-up state. Given diameter d and fill percentage p, the simulation minimizes (6) using Adam with gradient clipping to obtain the equilibrium profile.

Extracted quantities. From the converged profile we extract five measurable quantities (Figure 2 (right)): the peak height h; the radial and vertical coordinates (r_a, z_a) at the embroidery boundary; and the coordinates (r_b, z_b) of the point of minimum radial displacement just outside the boundary, which marks the transition from the buckled dome to the flat outer fabric.

Calibration procedure. To calibrate the material parameters, we fabricated 25 samples with parameters $(p, d) \in \{0.6, 0.7, 0.8, 0.9, 1.0\} \times \{20, 40, 60, 70, 90\}$, where p is fill percentage and d is patch diameter in millimeters. Instead of trying to fit the predicted profiles to the actual profiles, we compare designs using only these five keypoints. Seven material parameters ($w_{b,\text{emb}}$, $w_{b,\text{fab}}$, $k_{r,\text{emb}}$, $k_{r,\text{fab}}$, $k_{\theta,\text{emb}}$, $k_{\theta,\text{fab}}$, and $w_{\log}$) are then calibrated by minimizing the mean squared error between the simulated and experimentally measured values of (h, r_a, z_a, r_b, z_b) across the 25 specimens using differential evolution [22].

Figure 3 displays photographs of fabricated samples and simulated profiles with varying diameter and fill percentage. We observe an increase in both the height and size of the deformed structure as we increase the patch diameter (top). The bottom row shows how the profile evolves as the fill percentage changes. At lower fill percentages, patches form smoother, dome-like shapes. As fill percentage increases, deformation becomes more laterally distributed, producing flatter central regions and sharper boundary transitions. At high fill percentages, this results in a characteristic overhanging "mushroom-like" profile, where the embroidered boundary extends beyond the underlying fabric bend.

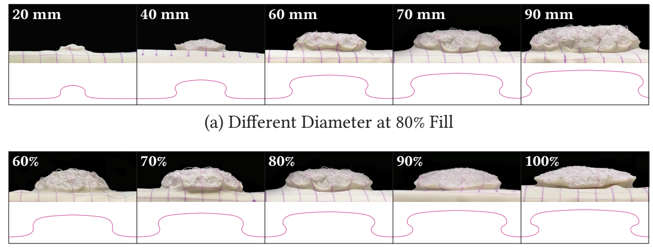

(a) Different Diameter at 80% Fill

(b) Different Fill Percentage at 70 mm diameter

Figure 3: Fabricated examples and simulated profile at different patch diameter (top) and fill percentage (bottom). Result shows that diameter affects size and height and fill percentage affects profile shape.

Figure 4 shows predicted height from densely sampled design parameters, revealing a positive non-linear relationship between fill percentage, diameter, and predicted height, and a regime where small size combined with low fill percentage leaves the embroidered region too compliant to overcome the fabric's elasticity, resulting in a near-flat configuration. We also characterize bistable switching forces across the design space, finding that switching force increases with both diameter and fill percentage, with their interaction providing control over actuation thresholds (Appendix B).

We validate this effect with fabricated examples at 50% fill (Figure 9 in Appendix). Lastly, we show that the tesselation resolution under the same fill percentage and diameter does not significantly impact the deformed geometry (Figure 10 in Appendix).

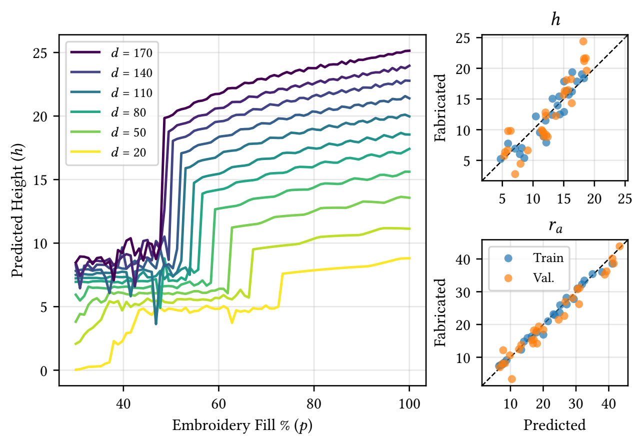

Figure 4: Simulated height h from densely sampled parameters (left, noise are due to numerical stability). Actual vs. Simulated height h (top-right) and perceived radius r_a (bottom-right) of 25 training (blue) and 28 validating (orange) fabricated examples.

5 Computational Design Pipeline

We develop an interactive design tool that supports an end-to-end workflow from garment-scale layout to fabrication-ready embroidery files. The tool enables users to parameterize and preview textile patches, connecting geometric design with predicted deformation behavior and fabrication constraints. This allows users to design in terms of desired deformation behavior rather than low-level embroidery geometry.

Design Mode. The workspace combines a 2D textile layout with a linked 3D deformation preview (Figure 5). The 2D canvas supports rectangular layouts and imported garment patterns (DXF), enabling interactive placement and parameter adjustment of circular patches.

Each patch is controlled by diameter and embroidery fill percentage, consistent with our characterization. Multiple patches can be composed across the textile layout to create larger designs. The 3D view provides real-time visualization of predicted deformation using our data-driven simulation model. To enable interactive performance, we precompute the model across the design space and query it at runtime as users adjust parameters.

The tool also supports inverse design: given target deformation height, the system suggests compatible parameter combinations, allowing users to efficiently explore the design space.

Design Variations. Beyond uniform patches, the tool supports spatially varying bistability within a single design. Users can combine regions with different fill percentages to control where bistable behavior occurs. This includes deliberately exploiting non-working regimes that do not produce strong bistability to create softer, compliant regions for artistic and expressive effects. For example, a high-fill central patch can be embedded within a lower-fill surrounding region to create a functional bistable element with a custom outer shape, enabling exploration of non-circular forms while preserving localized functionality.

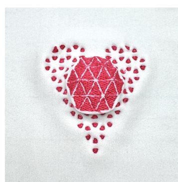

Fabrication Mode. Once a design is finalized, users transition to Fabrication Mode to generate embroidery output (Figure 11). The system groups patches into hoops using a bin-packing strategy that accounts for stretched patch dimensions and hoop margins, and computes stitching order to reduce interference between previously stitched regions and the hoop frame. A constraint panel checks fabrication feasibility, including hoop fit, minimum feature size, and proximity to fabric edges. Final designs are exported as standard embroidery files for direct fabrication.

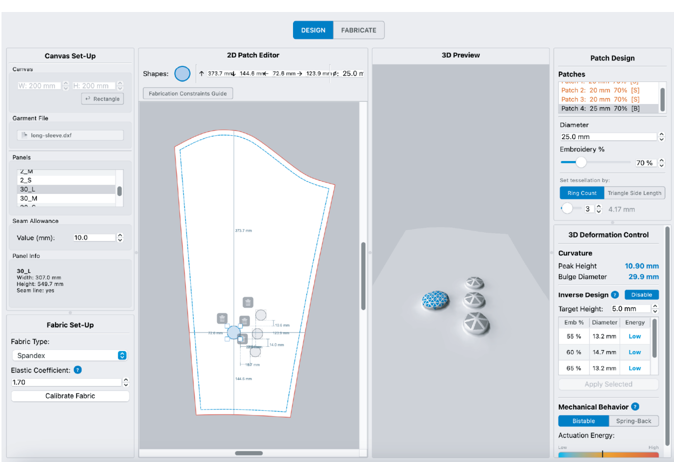

Figure 5: Design Mode of our UI, where users place and parameterize patches to control deformation and bistable behavior directly on garment layouts.

5.1 Model Validation

We evaluate the accuracy of our model by comparing predicted deformation with fabricated results across the parameter space. We generate two sets of validation designs using the UI. In the first, we sample random parameter pairs $d \in [15, 100]$ and $p \in [0.6, 1.0]$. In the second, we perform inverse design by specifying target deformation height h and boundary radius r_a and randomly selecting from the returned parameter combinations. A total of 28 designs are created and exported directly through the UI.

For each fabricated patch, we measure the five extracted quantities (h, r_a, z_a, r_b, z_b) using a fixed photography setup with orthogonal side views to minimize manual error, and compare against model predictions in Figure 4 (right). The model achieves high agreement in deformation height h and boundary radius r_a, with validation percentage errors of 24.6% and 15.8%, respectively (see Table 1 and Fig. 8 in Appendix for metrics across all quantities).

These results indicate that the model captures key deformation characteristics with sufficient accuracy to support real-time preview and inverse parameter selection within the design tool.

6 Applications

We demonstrate StitchSwitch through two applications that highlight how programmable surface deformation and bistability enable structural functionality and interaction in wearable systems (Figure 6). These examples show how the parameterized design space provides control over form and tactile input directly within textiles.

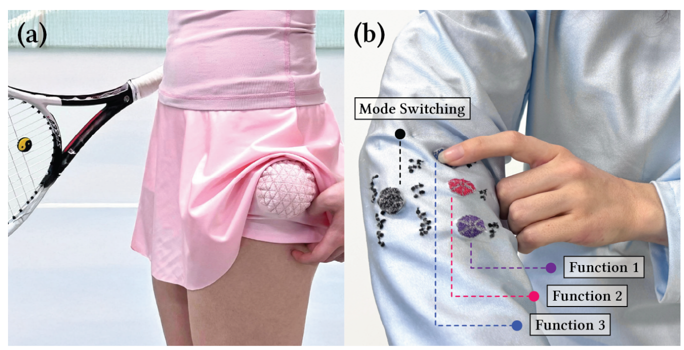

Figure 6: (a) A tennis skirt with a deformable pocket for ball storage, (b) a programmable garment interface with functional buttons and embroidered tactile labels.

6.1 Tennis Skirt with Deformed Pocket

We demonstrate garment-scale integration through a tennis skirt with an embroidered deformation-based pocket for holding a tennis ball (Figure 6a). A StitchSwitch patch is designed to form an outward deformation that creates a stable cavity, providing structural functionality directly in the fabric without requiring a separate sewn pocket.

To evaluate robustness under realistic use, we measured the pocket before and after a 1.5-hour tennis session followed by a wash-and-dry cycle. The pocket height remained stable (17.5 mm before and 17.8 mm after), with bistability preserved and no visible degradation (Figure 12 in Appendix).

6.2 Programmable Garment Interface

We demonstrate a programmable garment interface using embroidered patches as tactile input elements (Figure 6b). Tactile interfaces embedded directly into garments provide a pathway toward eyes-free interaction with everyday functions, building on prior work in tactile graphics and accessible textile fabrication [20].

We construct a forearm garment with an array of embroidered patches arranged as tactile buttons. The parameterized design space enables different tactile responses to be encoded directly into the textile. We use conductive thread as the bobbin thread during embroidery and integrate conductive pads beneath the textile layer to detect button state changes, an instance of the programmable conductive regions described in Section 3 (Figure 13 in Appendix).

This application illustrates how programmable textile deformation can support wearable interactions. We do not evaluate the interface with blind or low-vision participants; instead, we demonstrate the fabrication possibilities of combining tactile structures, conductive embroidery, and programmable deformation. Visual encoding through color and spatial layout supports button memorability, and the buttons are mapped to common shortcut functions (e.g., call, message, navigation).

7 Conclusion and Discussion

We present StitchSwitch, a computational design and fabrication system for programming surface deformation and bistability into embroidered textiles. By defining a compact, parameterized design space, we establish a predictable mapping from geometric design to deformation that supports an end-to-end design and fabrication workflow. Our applications illustrate how deformation mediates contact and interaction directly within textiles, opening up new possibilities for programmable textiles and wearable systems.

This work also opens several directions for further exploration. We observe that additional embroidery parameters, such as tension differences between the top and bobbin thread, influence mechanical behavior. When tensions are more balanced, patches exhibit more symmetric bistable behavior, while introducing differences creates asymmetry that biases the patch toward one stable configuration, enabling effects such as spring-back. In the Programmable Garment Interface, we leveraged this to combine bistable buttons with spring-back buttons that return to their original state. We also observe that factors such as tessellation resolution, thread weight, bobbin tension, and material properties of the thread affect bistability and deformation characteristics. These effects are not formally characterized in this work but suggest additional controllable dimensions in the design space for future work, including parameters that influence activation force and switching behavior.

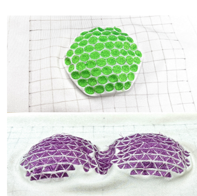

Another direction is exploring alternative tessellations, where preliminary tests with non-triangular symmetric patterns yield similar deformation behaviors, though full characterization remains future work (inline figure, top). Likewise, extending beyond circular patches to arbitrary geometries offers a promising direction for extending the design space (inline figure, bottom).

Acknowledgments

This work was supported by NSF 2327136, NSF 2319181, and a Sloan Research Fellowship. Claude (Anthropic) was used to provide support during parts of the code development process. ChatGPT (OpenAI) and Gemini (Google) were used to assist with writing tasks such as grammar checks, wording, and clarity revisions. All suggested changes were reviewed and included only after author evaluation and revision.

References

[1] Byoungkwon An, Ye Tao, Jianzhe Gu, Tingyu Cheng, Xiang 'Anthony' Chen, Xiaoxiao Zhang, Wei Zhao, Youngwook Do, Shigeo Takahashi, Hsiang-Yun Wu, Teng Zhang, and Lining Yao. 2018. Thermorph: Democratizing 4D Printing of Self-Folding Materials and Interfaces. In *Proceedings of the 2018 CHI Conference on Human Factors in Computing Systems* (Montreal QC, Canada) *(CHI '18)*. Association for Computing Machinery, New York, NY, USA, 1–12. doi:10.1145/3173574.3173834

[2] Zekun Chang, Yixuan Gao, Yuta Noma, Shuo Feng, Xinyi Yang, Kazuhiro Shinoda, Tung Ta, Koji Yatani, Tomoyuki Yokota, Takao Someya, Tomohiro Tachi, Yoshihiro Kawahara, Koya Narumi, Francois Guimbretiere, and Thijs Roumen. 2025. OriStitch: A Machine Embroidery Workflow to Turn Existing Fabrics into Self-Folding 3D Textiles. In *Proceedings of the ACM Symposium on Computational Fabrication (SCF '25)*. Association for Computing Machinery, New York, NY, USA, Article 21, 14 pages. doi:10.1145/3745778.3766666

[3] Tian Chen, Julian Panetta, Max Schnaubelt, and Mark Pauly. 2021. Bistable auxetic surface structures. *ACM Trans. Graph.* 40, 4, Article 39 (July 2021), 9 pages. doi:10.1145/3450626.3459940

[4] Tiffany Cheng, Yasaman Tahouni, Dylan Wood, Benjamin Stolz, Rolf Mülhaupt, and Achim Menges. 2020. Multifunctional Mesostructures: Design and Material Programming for 4D-printing. In *Proceedings of the 5th Annual ACM Symposium on Computational Fabrication* (Virtual Event, USA) *(SCF '20)*. Association for Computing Machinery, New York, NY, USA, Article 11, 10 pages. doi:10.1145/3424630.3425418

[5] David T. Farrell, Connor M. McCann, Antonio Elia Forte, Conor J. Walsh, and Katia Bertoldi. 2025. Programmable Surface Dimpling of Textile Metamaterials for Aerodynamic Control. *Advanced Materials* 37, 40 (2025), 2505817. arXiv:https://advanced.onlinelibrary.wiley.com/doi/pdf/10.1002/adma.202505817 doi:10.1002/adma.202505817

[6] Kate Glazko, Alexandra Portnova-Fahreeva, Arun Mankoff-Dey, Afroditi Psarra, and Jennifer Mankoff. 2024. Shaping lace: Machine embroidered metamaterials. In *Proceedings of the 9th ACM Symposium on Computational Fabrication* (Aarhus, Denmark) *(SCF '24)*. Association for Computing Machinery, New York, NY, USA, Article 7, 12 pages. doi:10.1145/3639473.3665792

[7] Ruslan Guseinov, Connor McMahan, Jesús Pérez, Chiara Daraio, and Bernd Bickel. 2020. Programming temporal morphing of self-actuated shells. *Nature Communications* 11, 1 (2020), 237. doi:10.1038/s41467-019-14015-2

[8] Ruslan Guseinov, Eder Miguel, and Bernd Bickel. 2017. CurveUps: shaping objects from flat plates with tension-actuated curvature. *ACM Trans. Graph.* 36, 4, Article 64 (July 2017), 12 pages. doi:10.1145/3072959.3073709

[9] Alice C Haynes and Jürgen Steimle. 2024. Flextiles: Designing Customisable Shape-Change in Textiles with SMA-Actuated Smocking Patterns. In *Proceedings of the 2024 CHI Conference on Human Factors in Computing Systems* (Honolulu, HI, USA) *(CHI '24)*. Association for Computing Machinery, New York, NY, USA, Article 517, 17 pages. doi:10.1145/3613904.3642848

[10] Yu Jiang, Alice C Haynes, Narjes Pourjafarian, Jan Borchers, and Jürgen Steimle. 2024. Embrogami: Shape-Changing Textiles with Machine Embroidery. In *Proceedings of the 37th Annual ACM Symposium on User Interface Software and Technology* (Pittsburgh, PA, USA) *(UIST '24)*. Association for Computing Machinery, New York, NY, USA, Article 63, 15 pages. doi:10.1145/3654777.3676431

[11] David Jourdan, Victor Romero, Etienne Vouga, Adrien Bousseau, and Mélina Skouras. 2022. Simulation of printed-on-fabric assemblies. In *Proceedings of the 7th Annual ACM Symposium on Computational Fabrication* (Seattle, WA, USA) *(SCF '22)*. Association for Computing Machinery, New York, NY, USA, Article 6, 11 pages. doi:10.1145/3559400.3562001

[12] David Jourdan, Mélina Skouras, Etienne Vouga, and Adrien Bousseau. 2022. Computational Design of Self-Actuated Surfaces by Printing Plastic Ribbons on Stretched Fabric. *Computer Graphics Forum* 41, 2 (2022), 493–506. arXiv:https://onlinelibrary.wiley.com/doi/pdf/10.1111/cgf.14489 doi:10.1111/cgf.14489

[13] Mina Konaković, Keenan Crane, Bailin Deng, Sofien Bouaziz, Daniel Piker, and Mark Pauly. 2016. Beyond developable: computational design and fabrication with auxetic materials. *ACM Trans. Graph.* 35, 4, Article 89 (July 2016), 11 pages. doi:10.1145/2897824.2925944

[14] Mina Konaković-Luković, Julian Panetta, Keenan Crane, and Mark Pauly. 2018. Rapid deployment of curved surfaces via programmable auxetics. *ACM Trans. Graph.* 37, 4, Article 106 (July 2018), 13 pages. doi:10.1145/3197517.3201373

[15] Luigi Malomo, Jesús Pérez, Emmanuel Iarussi, Nico Pietroni, Eder Miguel, Paolo Cignoni, and Bernd Bickel. 2018. FlexMaps: computational design of flat flexible shells for shaping 3D objects. *ACM Trans. Graph.* 37, 6, Article 241 (Dec. 2018), 14 pages. doi:10.1145/3272127.3275076

[16] Annika Muehlbradt, Gregory Whiting, Shaun Kane, and Laura Devendorf. 2022. Knitting Access: Exploring Stateful Textiles with People with Disabilities. In *Proceedings of the 2022 ACM Designing Interactive Systems Conference* (Virtual Event, Australia) *(DIS '22)*. Association for Computing Machinery, New York, NY, USA, 1058–1070. doi:10.1145/3532106.3533551

[17] Koya Narumi, Kazuki Koyama, Kai Suto, Yuta Noma, Hiroki Sato, Tomohiro Tachi, Masaaki Sugimoto, Takeo Igarashi, and Yoshihiro Kawahara. 2023. Inkjet 4D Print: Self-folding Tessellated Origami Objects by Inkjet UV Printing. *ACM Trans. Graph.* 42, 4, Article 117 (July 2023), 13 pages. doi:10.1145/3592409

[18] J. Panetta, M. Konaković-Luković, F. Isvoranu, E. Bouleau, and M. Pauly. 2019. X-Shells: a new class of deployable beam structures. *ACM Trans. Graph.* 38, 4, Article 83 (July 2019), 15 pages. doi:10.1145/3306346.3323040

[19] Jing Ren, Aviv Segall, and Olga Sorkine-Hornung. 2024. Digital Three-dimensional Smocking Design. *ACM Trans. Graph.* 43, 2, Article 14 (Jan. 2024), 17 pages. doi:10.1145/3631945

[20] Margaret Ellen Seehorn, Claris Winston, Bo Liu, Gene S-H Kim, Emily White, Nupur Gorkar, Kate S Glazko, Aashaka Desai, Jerry Cao, Megan Hofmann, and Jennifer Mankoff. 2025. Beyond Beautiful: Embroidering Legible and Expressive Tactile Graphics. In *Proceedings of the 27th International ACM SIGACCESS Conference on Computers and Accessibility (ASSETS '25)*. Association for Computing Machinery, New York, NY, USA, Article 26, 21 pages. doi:10.1145/3663547.3746336

[21] Aviv Segall, Jing Ren, Amir Vaxman, and Olga Sorkine-Hornung. 2024. Fabric Tessellation: Realizing Freeform Surfaces by Smocking. *ACM Trans. Graph.* 43, 4, Article 89 (July 2024), 20 pages. doi:10.1145/3658151

[22] Rainer Storn and Kenneth Price. 1997. Differential Evolution – A Simple and Efficient Heuristic for global Optimization over Continuous Spaces. *Journal of Global Optimization* 11, 4 (01 Dec 1997), 341–359. doi:10.1023/A:1008202821328

[23] Hye Jun Youn, Jun Kyu Choe, SooYeon Ahn, Marcello Tania, Serena Xin Wei Sara, and Hiroshi Ishii. 2026. PixBric: Precision Morphological Control of Pre-Stretched Fabrics Through Tessellated Primitive Geometries. In *Proceedings of the Twentieth International Conference on Tangible, Embedded, and Embodied Interaction (TEI '26)*. Association for Computing Machinery, New York, NY, USA, Article 20, 15 pages. doi:10.1145/3731459.3773316

[24] Chao Yuan, Shengqi Dang, Xuejiao Ma, and Nan Cao. 2026. FreeShell: A Context-Free 4D Printing Technique for Fabricating Complex 3D Triangle Mesh Shells. *ACM Trans. Graph.* 45, 2, Article 21 (Jan. 2026), 12 pages. doi:10.1145/3778349

A Fabrication Details

We fabricate StitchSwitch patches using standard machine embroidery on pre-stretched elastic fabric. Unlike conventional embroidery workflows, which aim to stabilize fabric by minimizing stretch, our process intentionally maximizes and preserves pre-strain during embroidery. The fabric is placed over a single sheet of water-soluble stabilizer and stretched uniformly in both directions before being secured within an embroidery hoop. We use a drawn grid reference and pinning to ensure even stretching, achieving approximately 170% elongation (elastic coefficient ≈ 1.7).

Embroidery is then applied directly onto the tensioned fabric, forming a multilayer structure consisting of top thread, base fabric, stabilizer, and bobbin thread. While this layered construction contributes to local stiffness, deformation behavior in our system is governed primarily by the spatial distribution of stitched geometry rather than layer asymmetry. After embroidery, the fabric is released from the hoop and rinsed to dissolve the stabilizer, allowing the fabric to relax and the embroidered regions to deform out of plane.

We fabricate patches using a Janome MemoryCraft 550E embroidery machine on four-way stretch spandex with water-soluble stabilizer. Our empirical characterization uses standard 40-weight polyester threads. We observe similar qualitative deformation trends with 60-weight threads, though deformation magnitude and saturation behavior vary due to differences in effective stiffness of the embroidered region. We do not systematically characterize these effects. The fabrication process also supports variation in thread type and configuration, including conductive threads and mid-design thread changes, enabling functional extensions such as sensing. While thread tension influences mechanical behavior, we do not explicitly characterize this effect and discuss it further in Section 6.

B Bistability Characterization

We characterize the switching force required to transition StitchSwitch patches between their two stable states across the design space. For each sample, we apply force normal to the patch center using a contact plate sized according to the patch diameter and measure the minimum weight required to induce bistable switching. Slotted weights are incrementally added until the patch transitions to the opposite stable configuration. The resulting force is computed from the applied mass and gravity.

We measure switching forces across the same design space used for model calibration, with patch diameters ranging from 20–90 mm and fill percentages from 0.6–1.0. The tested forces range from 0.04–0.77 N across contact areas of 0.44–15.9 cm^2, all within the range of hand actuation.

To model the relationship between design parameters and switching force, we fit a second-order polynomial model using the 25 calibration samples and evaluate it on the 28 validation samples. The model achieves $R^2 = 0.95$ on the training set and $R^2 = 0.80$ on the validation set, with a validation mean absolute error of 0.06 N.

The fitted model reveals that switching force increases with both patch diameter and fill percentage, with an interaction effect between the two parameters. This relationship enables designers to select patches with different actuation thresholds while maintaining the same underlying fabrication primitive.

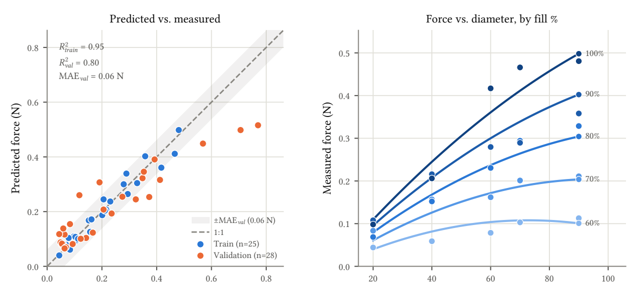

Figure 7: Bistable force model characterization. Left: predicted vs. measured switching force on the train and validation sets. Right: measured force vs. patch diameter across fill percentages, showing the diameter×fill interaction the model captures.

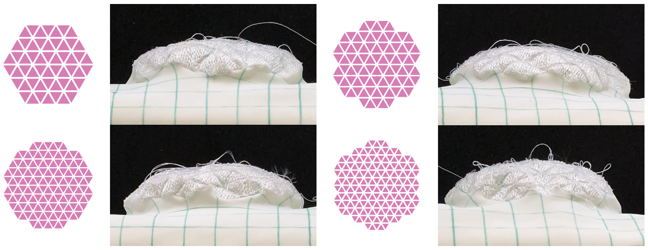

Figure 10: Embroidery pattern and fabricated results of different tesselation of the same diameter and fill percentage. The result shows no visual difference in the geometry of the deformed fabric.

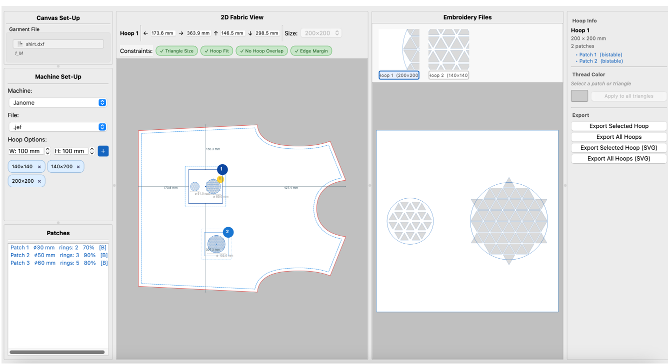

Figure 11: Fabrication Mode interface showing hoop optimization for multiple patches and the corresponding selected hoop layout for embroidery.

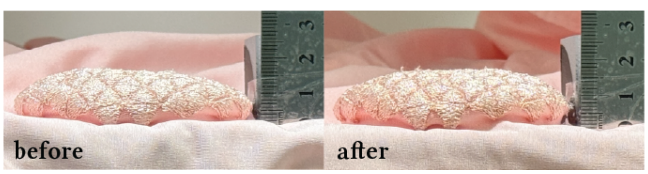

Figure 12: Tennis pocket before and after a 1.5-hour tennis session and wash-and-dry cycle. Deformation height remained stable (17.5mm before, 17.8mm after), with bistable switching preserved and no visible degradation.

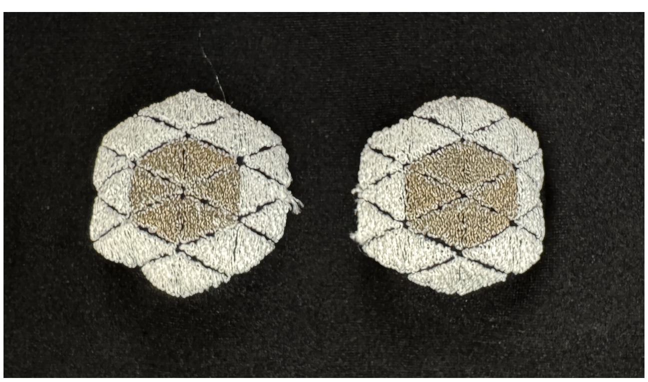

Figure 13: Conductive thread integration within StitchSwitch patches. Selective placement of conductive embroidery thread enables programmable interaction regions while preserving the underlying bistable structure.

C Additional Results

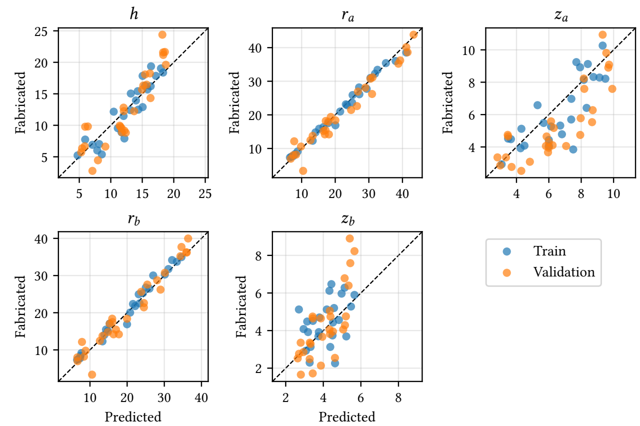

Figure 8: Actual vs Simulated of five measurable quantity. See Fig 2 (right) for definition of each quantity.

	Error (%)		MAE (mm)	
Quantity	Train	Val.	Train	Val.
h	14.7	24.6	1.44	2.23
r_a	4.5	15.8	0.87	1.82
z_a	20.4	31.7	1.09	1.45
r_b	6.1	16.2	1.05	1.80
z_b	22.9	25.8	0.93	0.99

Table 1: Percentage error and mean absolute error (MAE) between simulated and measured deformation quantities for the training and validation sets.

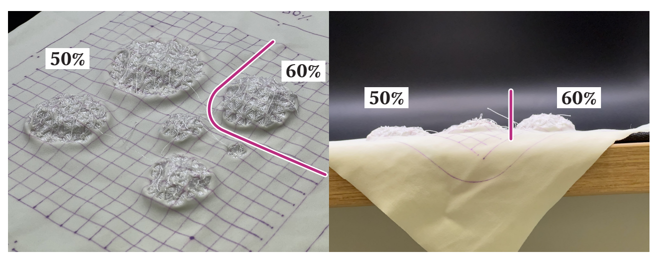

Figure 9: Embroidered samples with 50% and 60% fill. At lower diameter and fill percentage, we have near flat configurations as the sparse patterns do not have enough stiffness to maintain their shape.